Considering different criteria for minimizing torsional response of asymmetric structures under near-fault and far-fault excitations

Hamzeh Shakib[1], **Abbas Ghasemi**[2]

[1]Professor, Department of Civil Engineering, Tarbiat Modares University, Tehran, Iran
[2]Ph.D. Candidate, Department of Civil Engineering, Tarbiat Modares University, Tehran, Iran

Abstract: *An attempt has been made to explore the general trends in the seismic response of plan-asymmetric structures when subjected to near-fault and far-fault ground motions. Systems with structural wall elements in both orthogonal directions considering actual and common nonlinear behavior under bi-directional excitation were studied. Idealized single-storey models with uni-axial eccentricity were employed. The main findings are: The rotational response trend considering actual behavior method would be different from common behavior method assumption, when the system subjected to near-fault motions. In the former case, the minimum rotational response could be achieved, when stiffness and strength centers are located on opposite side of the mass center. In the latter case, stiffness eccentricity determines the minimum and maximum rotational response. General trends in the rotational demand for far-fault motions, considering two type behavior assumptions, are similar to the last case. Moreover, in near-fault motions, when stiffness and strength centers are located on opposite side of the mass center, stiff side displacement demand would be greater than that soft side which is contrary to the conventional guidelines. While, in far-fault motions similar to near-fault motions which stiffness and strength centers are located on one side of the mass center, displacement demand would be according to conventional guidelines.*

Keywords: *Near-fault, torsional response, asymmetric structures, far-fault*

1. Introduction

Asymmetric buildings with centers of stiffness and strength being different from the center of floor mass, respond to earthquake excitation in coupled modes, producing both lateral and torsional motions. Such buildings as reported by many researches [1-6] are highly vulnerable due to the torsional response. The position of the stiffness and strength centers towards the floor mass center could highly affect the torsional response. In the past two decades, many studies have been carried out on asymmetric structures. Most of these studies are concentrated on the effects of structural systems as well as the earthquake characteristics on the responses. Moreover, in most of these studies, multi-storey structures have been generally idealized as one-storey structures, and the linear and nonlinear behaviors of the idealized structural systems are studied. The above studies show that the response of structures with linear assumption is significantly related to the natural lateral period, torsional frequency to lateral frequency ratio, and the stiffness eccentricity. On the other hand, as soon as the resistant elements enter into plastic phase, stiffness of elements change, and consequently, stiffness center and natural frequency change in the nonlinear behavior. Hence, system nonlinear responses related to the above elastic parameters as well as the number, position, direction and yield strength of resistant elements. The studies on the asymmetric buildings with a nonlinear behavior are usually based on the conventional guidelines for strength assignments which are stiffness distribution

based.

Paulay[5] showed that the yield displacement of shear walls depend only on the material properties, such as limiting strain, and the geometry of the components of structure elements . For design purposes generally yield displacements considered to be independent of the strength assigned to components or elements. Since in a plastic mechanism, the sequence of the onset of the components yielding, is independent of their strength, within rational limits, strengths may be assigned to components in the way that suits the designer's intentions. With re-defined stiffness, relating freely chosen strengths to strength-independent yield displacements enables a more realistic assessment of elements or of a system to be made. Tso and Myslimaj [6], proved that the yield displacement distribution-based strength assignments between resisting elements, does not require the knowledge of stiffness distribution prior to strength assignment. They concluded that, when strength and stiffness centers are two sides of the mass center, minimum torsional response could be obtained. Sommer and Bachmann [7] tried to invent a new designing method based on the concept of yield displacement of shear wall sections. They calculated ultimate deformation and strength elements on the base of stiffness and strength eccentricity and allowable ductility and story-drift criteria. Stathopoulos and Anagnostopoulos [8] considered the displacement ductility demands in reinforced concrete frames and finally concluded that ductility demand in stiff side of one – storey structures is greater than the soft side; however the soft side ductility demand of multi-storey structures is greater than their stiff side. This conclusion is in contrast with the guideline codes. Perus and Fajfar [9] considered torsional effects in elastic and inelastic behavior. They comprehended that system behaviors with mass eccentricity are very similar to systems with stiffness eccentricity which their stiffness and strength depend on each other. In addition, though maximum rotation and maximum displacement aren't simultaneous, these two parameters depend on each other.

Near-fault researches focus on two classes. The first class is about different parameters and characters of near-fault motions. Researches on near-fault records simulation are also categorized in this group. The second class of this studies relate to considering the effects of near-fault records on the behavior of structures. Somerville [10] presented equations between fault-normal component pulse period of near-fault motion "T_p" and moment magnitude. Furthermore he presented the equitation between peak ground velocity (PGV) and the shortest distance from fault.

Alavi and krawinkler [11] considered equivalent pulse, which has comparable effect with near-fault motions on structure response. Mavroeidis and Papageorgiou [12] suggested a mathematical model for describing dynamic response of SDOF systems as a function of the input parameters. Furthermore they studied elastic and inelastic response of SDOF systems under near-fault motions. Edrik and Durukal [13] idealized long period pulse of near-fault records with sinusoidal model. Chopra and Chintanapakdee [14] considered elastic and inelastic response of SDOF systems in acceleration-, velocity-, and displacement-sensitive regions of response spectrum. They concluded that the velocity-sensitive region for near-fault motions is much narrower, and the acceleration-sensitive and displacement-sensitive regions are much wider, compared to far-fault motions. Moreover, the strength reduction factor, R_y, and the ratio $\frac{u_m}{u_0}$ of

Table 1 near-fault records and their characteristics

earthquake	Record (station)	Fault distance (km)	component	PGA (g)	PGV (cm/s)	PGD (cm)	$\frac{\dot{u}_g}{\ddot{u}_g}$	$\frac{u_g}{\dot{u}_g}$
Northridge	NR94newh (Newhall)	7.1	Newhall- 90	0.583	75.5	17.57	0.13	0.23
			Newhall- 360	0.59	97.2	38.05	0.17	0.39
Northridge	NR94rrs (Rinaldi)	7.1	Rinaldi- 228	0.838	166.1	28.78	0.20	0.17
			Rinaldi- 318	0.472	73	19.76	0.16	0.27
Northridge	NR94spva (Sepulveda)	8.9	Sepulveda- 270	0.753	84.8	18.68	0.11	0.22
			Sepulveda- 360	0.939	76.7	14.95	0.08	0.19
Northridge	NR94scs (Converter)	6.2	Converter- 52	0.612	117.4	53.47	0.20	0.46
			Converter- 142	0.897	102.8	46.99	0.12	0.46
Northridge	NR94sylm (Olive)	6.4	Olive- 90	0.604	78.2	16.05	0.13	0.21
			Olive- 360	0.843	129.6	32.68	0.16	0.25
Northridge	NR94sce (East)	6.1	East- 18	0.828	117.5	34.22	0.14	0.29
			East- 288	0.493	74.6	28.69	0.15	0.38
Erzincan	EZ92erzi (Erzincan)	2	Erzinkan- 90	0.515	83.9	27.35	0.17	0.33
			Erzinkan- 0	0.496	64.3	22.78	0.13	0.35
Chi- chi Taiwan	CH92tcu52 (Tcu-52)	0.24	Tcu52- N	0.419	118.4	246.15	0.29	2.08
			Tcu52- W	0.348	159	184.42	0.47	1.16
Chi- chi Taiwan	CH92tcu68 (Tcu-68)	1.09	Tcu68- N	0.462	263.1	430	0.58	1.63
			Tcu68- W	0.566	176.6	324.11	0.32	1.84

deformations of inelastic and elastic systems are similar for the two types of motions. Alavi and krawinkler [11] evaluated the effects of near-fault ground motions and equivalent pulses on the structural response. They illustrated that in structures with a period longer than the pulse period, early yielding occurs in higher stories but the high ductility demands migrate to the bottom stories as the ground motion become more severe. When period of structure is shorter than the pulse period, the maximum demand always occurs in the bottom stories.

So far, the response behavior of torsional systems subjected to near-fault ground motion has not been evaluated. This study considers specifications of both fault-normal and fault-parallel components and their effects on the seismic responses of asymmetric structures. In the structure element model, shear walls are the resistant elements, with different distribution of strength and stiffness obtained with due attention to the new concepts of nonlinear behavior and assigning strength to resistant elements. The effects of common code and actual system material behaviors on the responses are also taken into consideration. Consequently ductility, displacement, and rotation demands of stiff and soft sides with due attention to effects of near-fault and far-fault records would be considered.

2. Ground Motion Data

In order to compare the effects of near-fault earthquake ground motions on rotation and displacement demands, two groups of records consisting of near-fault and far–fault records are selected with S_D soil condition as per NEHRP[15]. The set of 9 near-fault ground motions used in this study are listed in Table 1. For each record the peak ground acceleration, $\ddot{u}_g$, the peak ground velocity,

Table 2 far-fault records collection and their characteristics

earthquake	station	Fault distance (km)	component	PGA (g)	PGV (cm/s)	PGD (cm)	$\frac{\dot{u}_g}{\ddot{u}_g}$	$\frac{u_g}{\dot{u}_g}$
Imperial valley	victoria	54.1	Victoria- 75	0.122	6.4	2.09	0.053	0.33
			Victoria- 345	0.167	8.3	1.05	0.051	0.126
Loma prieta	City hall	28.2	City hall- 90	0.247	38.5	17.83	0.158	0.463
			City hall- 180	0.215	45	26.1	0.213	0.58
Loma prieta	Sunny vale	28.8	Sunny- 270	0.207	37.3	19.11	0.184	0.514
			Sunny- 360	0.209	36	16.9	0.176	0.472
Loma prieta	Slac lab	36.3	Slac- 270	0.194	37.5	9.96	0.197	0.27
			Slac- 360	0.278	29.3	9.72	0.107	0.334
Loma prieta	Halls valley	31.6	Halls- 0	0.134	15.4	3.3	0.117	0.21
			Halls- 90	0.103	13.5	5.46	0.134	0.407
San fernando	Holly wood	21.2	Holly- 90	0.21	18.9	12.4	0.092	0.652
			Holly- 180	0.174	14.9	6.25	0.087	0.42
Imperial valley	Elcentro	12	Elcentro- 180	0.313	29.8	13.32	0.097	0.44
			Elcentro- 270	0.215	30.2	23.91	0.143	0.8

$\dot{u}_g$,and the peak ground displacement , u_g, are presented. In order to compare the characteristics of near-fault and far-fault ground motions, it is also considered the set of 7 records of far-fault motions in Table 2. Comparing fault-normal component with fault–parallel component of the selected near-fault earthquake ground motions, ($u_g/\dot{u}_g$) and ($\dot{u}_g/\ddot{u}_g$) ratios are presented in Table 1. As it can be seen in Table 1 the PGA, PGV and PGD of fault-normal components are generally greater than fault-parallel components. However, in some of the selected near-fault earthquake ground motions, like: NR94spva, NR94scs, CH92t68 records, PGD values of fault-parallel components are greater than fault-normal components.

In order to compare the pseudo velocity spectra of fault-normal and fault-parallel components of the near-fault motions figure-1 is presented as a logarithmic plot. The idealized version of the response spectrum was constructed according to the procedures described in reference [16], where the spectrum is divided logically into three period ranges. As it can be seen from the figure, spectra are divided to acceleration-sensitive, velocity-sensitive and displacement-sensitive regions whereas the lines are not shown. The period between acceleration and velocity regions have direct relationship with $\dot{u}_g/\ddot{u}_g$ ratio, so when this ratio increases, acceleration-sensitive region would be wider and therefore it is expected that the drift of structure would be larger. In the selected earthquake cases, it is observed that for earthquake components that have a larger PGV and PGD, the $\dot{u}_g/\ddot{u}_g$ ratio would be higher and consequently the drift of structures would be larger. Furthermore, acceleration-sensitive region is wider and velocity-sensitive region is narrower in fault-normal components as compared to fault-parallel components.

Figure 2 showed acceleration and velocity elastic response spectra for both fault-normal and fault-parallel components of two near-

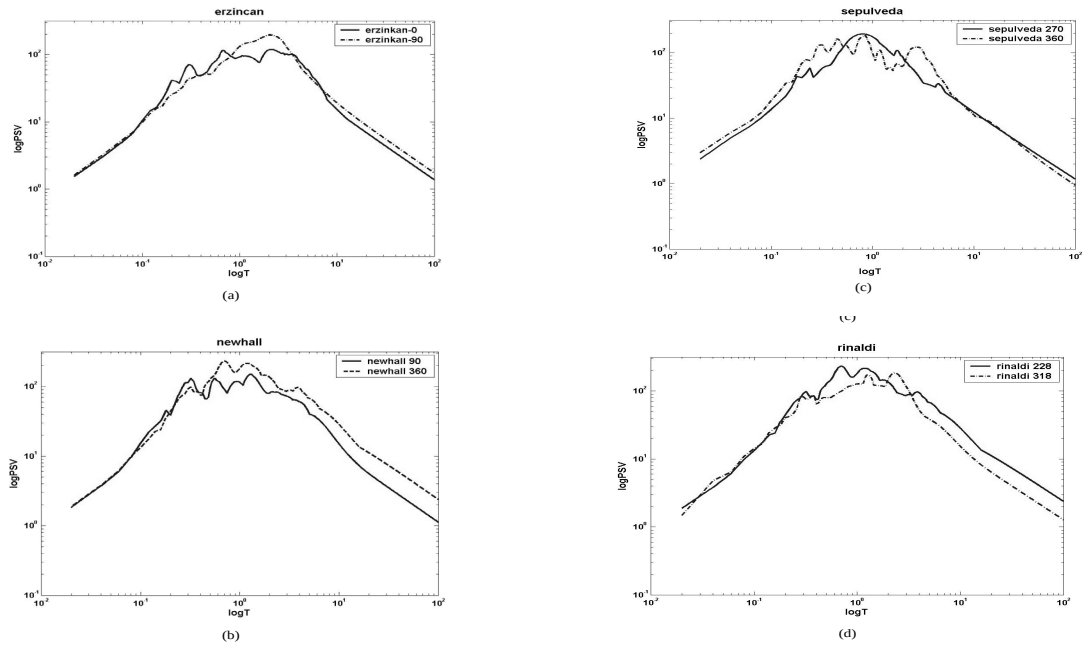

Fig.1 comparison pseudo velocity spectra of fault-normal and fault-parallel components of near-fault motion recorded at (a) Erzincan station (b) Newhall station (c) Sepulveda station (d) Rinaldi station

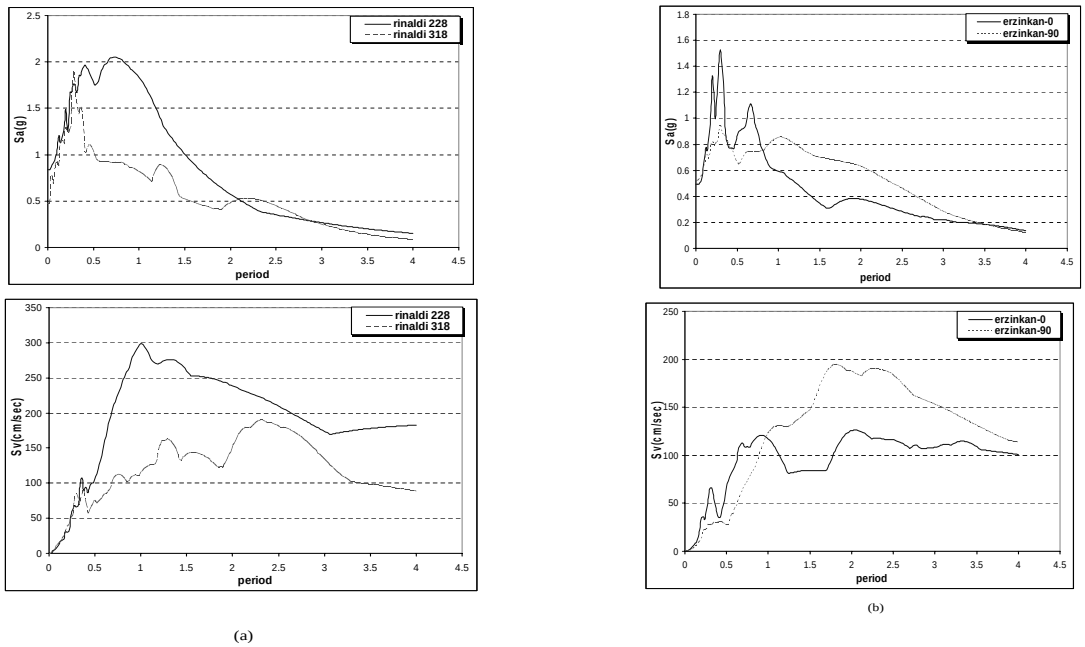

Fig.2 comparison acceleration, velocity response spectra's of fault-normal and fault-parallel components of (a) Rinaldi station (b) Erzincan station

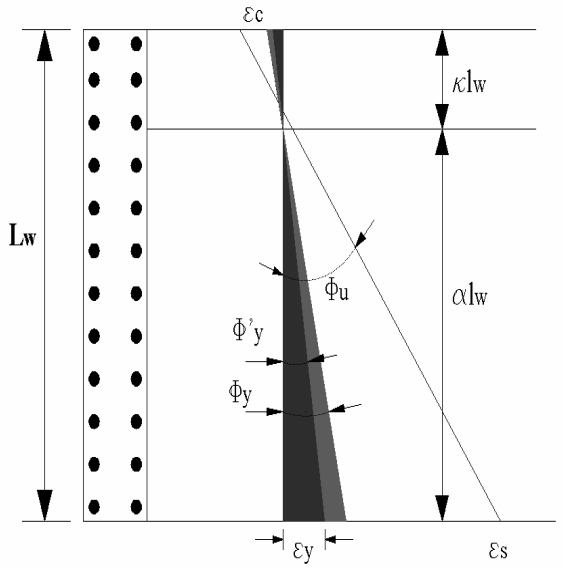

Fig.3 compressive strain and curvature of shear wall section

fault ground motions. The other specifications of near-fault earthquake ground motions are the difference between displacement, velocity and acceleration response spectra of fault–normal and fault–parallel components. Generally, in the fault–normal component, displacement, velocity and acceleration response spectra values are larger than fault-parallel components. However, in some of the response spectra of the near-fault earthquake ground motions the above characteristics are not observed. Such as, NR94newh record, PGA, PGV and PGD values of fault-normal components are larger as compared with fault–parallel components while the acceleration response spectra of fault-parallel components is larger than acceleration response spectra of fault-normal components. In NR94spva record, velocity and displacement spectra values of fault-normal components are smaller than fault-parallel components while fault–normal acceleration spectra are larger than fault-parallel component. In NR94scs record, acceleration and velocity spectra values of the fault-parallel components are larger than fault-normal ones. Moreover, in NR94sce record, the velocity spectra and in EZ92erzi record, the acceleration spectra, fault-parallel components have preference over fault-normal components. However, generally fault-normal spectra values are mostly larger than fault-parallel spectra values.

3. Nonlinear Behavior of Shear Walls

Many researchers such as "Paulay" [5] and "Pristely and kawalsky" [17] carried out a number of studies in this field. The ductile behavior of a wall is predominantly influenced by the response of the base section. As Fig. 3 shows ϕ'_y is the yield curvature of section, which is evaluated in standard texts. The yield strength, M_y, of the section and the corresponding base shear, V_y, developed at the onset of yielding at the extreme tension fiber, are associated with extensive cracking of the concrete. The wall section response under monotonic force application up to this level is strongly nonlinear. However, after the removal of the yield force, V_y, and its re-application, cyclic elastic response will be close to linear. Hence, in a seismic design, the linear

moment-curvature response at the base is a realistic measure of the flexural stiffness, also termed flexural rigidity, of a thoroughly checked wall section. Bilinear moment-curvature modeling implies that yield curvature, ϕ'_y, is extrapolated to the level when the nominal flexural strength of the section, M_n, is attained. The associated curvature will be subsequently referred to as the nominal yield curvature, ϕ_y, as shown in figure 3. In a routine design it is more convenient to relate deformations to the nominal strengths rather than the yield strengths. Once the nominal yield curvature at the base section of the wall component is established, the nominal yield displacement, for example at the top of the wall, is readily estimated by:

$$\Phi'_y = \varepsilon_y / (0.75 l_w) \quad , \quad \Phi_y = \left(\frac{M_n}{M_y}\right)\Phi'_y \qquad (1)$$

$$\therefore \Delta_{yi} = C \Phi_{yi} h_{wi}^2$$

Where ε_y is the yield strain of the reinforcing steel, L_w is the length of the shear wall and h_w is the shear wall height. "C" is a coefficient quantifying the effect on deflection of the pattern of applied lateral forces. For example, for the commonly used lateral static design forces in form of an inverted triangle, then:

$$\Delta_{yi} = 11 V_{ni} h_w^3 / (60 E_C I_e)_i \quad , \quad M_{ni} = 2 V_{ni} h_w / 3 \qquad (2)$$

$$\therefore \Delta_{yi} = (11/40) \Phi_{yi} h_w^2$$

It may be concluded that the yield displacement of a cantilever component is inversely proportional to its length, l_w. This important relationship may be effectively used in the design process, particularly when at an early stage displacement ductilities need to be estimated. Contrary to the traditional definition, based on the flexural rigidity of a prismatic component, E_cI_e, stiffness is proportional to the strength as provided in the wall component to be constructed. Using by bilinear simulation:

$$K_i = \frac{V_{ni}}{\Delta_{yi}} \qquad (3)$$

Rotenberg [18] evaluated seismic shear of ductile cantilever walls in multi-storey structures. He considered the distribution of seismic basic shear demand on ductile flexural cantilever walls. It is shown that the base shear force demand depends on the sequence of hinge formation at the wall bases. Hence, the routine elastic approach in which the shear forces are allocated per relative flexural rigidity or to moment capacity at the wall base may appreciably underestimate the shear force demand on the walls, particularly the shorter ones.

4. Structural System

Figure 4 presents the plan of an idealized one-storey building. The generic building model consists of a single rectangular concrete deck. The deck is supported by five reinforced concrete flexural wall elements in y-direction, and two equal wall elements at the edges in x-direction, as shown in the figure. With the idea that the yield displacements of wall elements can be determined from architectural drawings, the yield displacement distribution of the structure is known. The asymmetry of such a distribution is characterized by the location of the center of the yield displacement in relation to mass center. Using plastic mechanism analyses on a number of example structures [5] and focusing on the displacement ductility demand on the elements, it was concluded that, within rational limits, strength can be assigned to the elements in any way that suits the designer's intentions. A desirable strength distribution

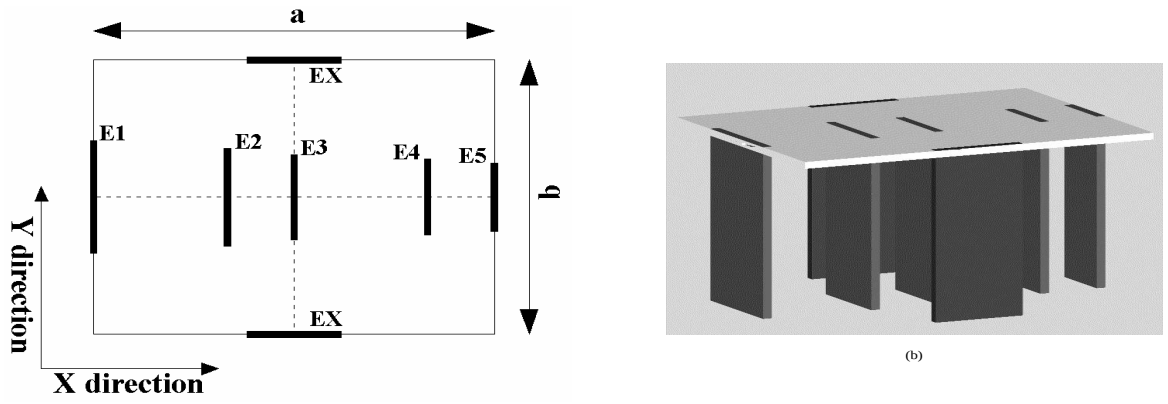

Fig.4 arrangement of resisting element in (a) plan and (b) three dimension

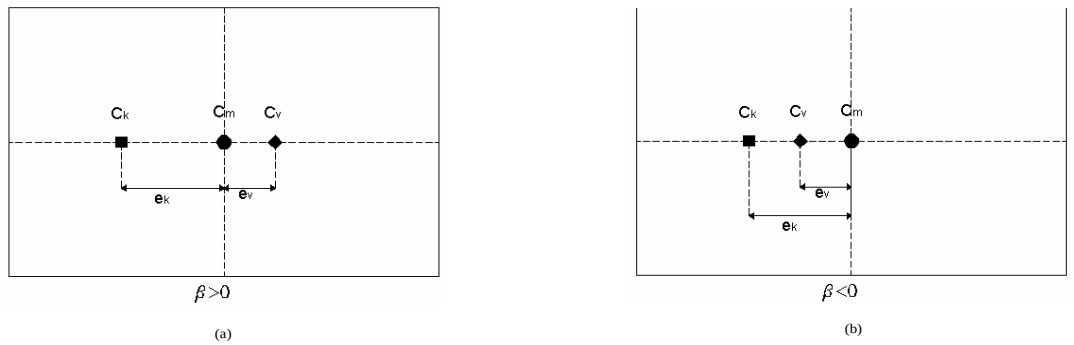

Fig.5 location of stiffness and strength centers (a) opposite side of the mass center (b) one side of the mass center

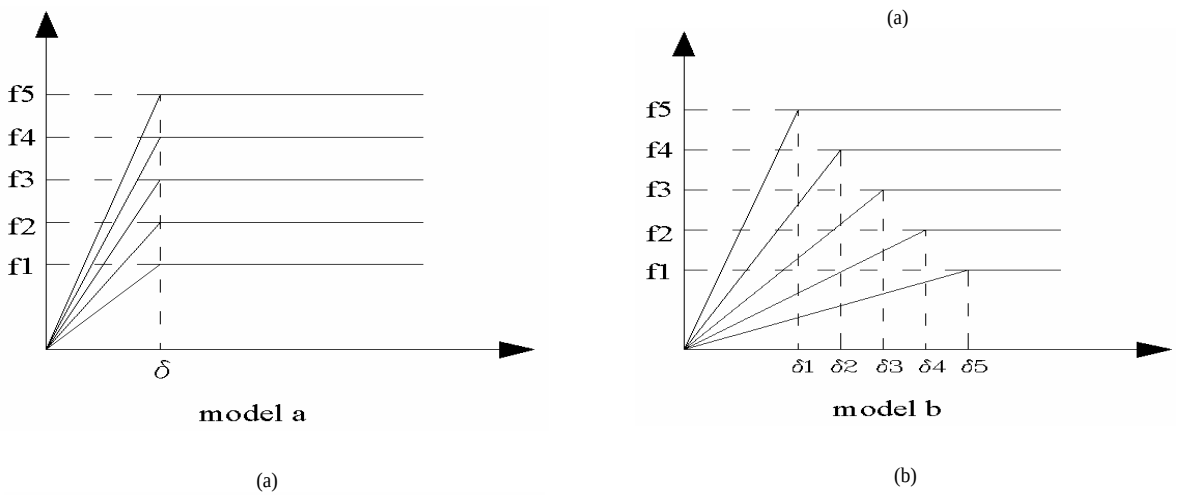

Fig.6 comparison nonlinear behavior methods (a) common "model a" and (b) actual "model b"

leads to establish strength centers that with due attention to the relation of stiffness to strength, different stiffness centers are created. Reference [6] favors a 'balanced CV-CR location' criterion to minimize the rotational response of asymmetric structures. Their proposed procedure suggests that the strength distribution should have a similar shape as the yield displacement distribution, modified by a parameter β be chosen by the designer. A continuum approach is used to accommodate systems having different numbers of resisting elements. Connecting the continuous model and the model with discrete resisting elements is based on the concept tributary area equivalence. Magnitudes of the yield displacement of the lamina at mass center, left and right edges are the basis parameters in the yield displacement distribution. Strength distribution have a similar shape as the yield displacement distribution that the basis parameter in distribution are determined by the following two conditions: (a)- the strength eccentricity is related to the yield displacement eccentricity by the relation "$e_v=\beta\, e_D$"; (b)-the radius of gyration for both strength and yield displacement are equal. In the above equation, e_v is the strength eccentricity, e_D is the yield displacement eccentricity and β is the parameter which can be chosen by the designer. On this base, the location of stiffness and strength centers for different strength distributions would appear as shown in figure 5. By choosing $\beta > 0$, the strength and stiffness centers are located on opposite sides of the mass center. While $\beta < 0$ will lead the strength and stiffness centers are located on one side of the mass center. $\beta = 0$ will give a system with zero strength eccentricity, and for $\beta = 1$ the system will lead to small or zero stiffness eccentricity. In order to consider variations of structural period on responses changing yield displacement and consequently changing height or length of wall element would be needed.

5. Numerical Study

In this study, nonlinear behavior of reinforcing steel is assumed to be bilinear, non-degrading hysteresis model with 3% strain hardening. The yield strain of the reinforcing steel (ε_y) is taken as 0.002 and the reinforcing steel yield strength (f_y) equals 4000 kg/cm^2. In addition concrete compressive nonlinear behavior is assumed to be bilinear with decreasing strength. Using elasto-plastic modeling to represent the force-displacement relationship of wall elements, five elements that have different dimension would have force-displacement plots as those shown in figure 6(a). Strength distributions between wall elements are basis on ratios of elements stiffness while the stiffness of elements related only to section dimension. Since strength to stiffness ratio in all elements is similar, all elements would have equal yield displacement so that the elements enter into plastic phase simultaneously. Mentioned behavior state labeled as common behavior method. An increase of strength will lead to an increase of yield displacement, but the stiffness of the element remains unchanged. Based on researches on nonlinear behavior, mentioned in previous sections, the force-displacement relationship of wall elements may be considered as bilinear, and their yield displacements depend only on material properties and the geometry of the elements. For seismic design purposes, the yield displacement may be considered to be independent of strength and can be determined prior to strength assignment. The force-displacement relationship for five elements with different dimensions would appear as shown in figure 6(b). With the yield

Table 3 arrangement of stiffness and strength centers considering common and actual behavior methods

model	Stiffness eccentricity (actual method)	Strength eccentricity (actual method)	Stiffness and Strength eccentricity (common method)
β = -0.5	-9.08%	-3.00%	-9.08%
β = -0.25	-7.64%	-1.50%	-7.64%
β = 0	-6.20%	0.00%	-6.20%
β = 0.25	-4.72%	1.50%	-4.72%
β = 0.5	-3.24%	2.99%	-3.24%
β = 0.75	-1.72%	4.49%	-1.72%
β = 1	-0.18%	5.99%	-0.18%

displacement remaining constant for each element, the stiffness and strength become dependent parameters. This behavioral state is labeled as actual behavior method. Considering a reinforced concrete section, with respect concrete fibers and steel fibers, it was concluded that plasticity theory does a mediocre job of modeling reinforced concrete for monotonically increasing loads, and a poor job for cyclic loads. On this basis, for vertical axial/bending behavior the total cross section of the cantilever will usually be divided into a number of fiber elements. The push-over analysis is carried out in order to control the stiffness and strengths of each wall elements.

Uncoupled lateral and uncoupled torsional periods are defined as the fundamental periods of the corresponding symmetric system. By changing the yield displacement of the idealized structural model, uncoupled lateral fundamental periods such as, 0.62, 1.0, 1.5, 2.0, 2.5 and 3 sec is derived. In this study the ratio of torsional frequency to lateral frequency is so selected to be, 0.75, 1.0, 1.5 and 2.0. Actual and common behavior methods were considered in structural models and for every behavior method, seven models were used which defined positions of strength and stiffness centers in relation to mass center. As afore-mentioned, the designer could define β parameter. Seven models are related to the different values of β parameter. In table No. 3, seven models with different stiffness and strength eccentricity are used. Strengths are distributed among the resisting elements Based on the β parameter. Since the yield displacement of the elements is unique, according to equation 3 the stiffness of each element is defined. So, strength, yield displacement and stiffness which are the major behavior parameters could be defined in each model.

5.1. "Ω" Frequency Ratio Consideration on Rotation Demands

Actual and common behavior methods are considered to compare "Ω" frequency ratio effects on responses. "Ω" Is the uncoupled torsional frequency to the uncoupled lateral frequency and given as the following:

$$K_{\theta R} = \sum_{i=1}^{N} k_{yi}(x_i - e)^2 + \sum_{i=1}^{N} k_{xi} y_i^{\,2} \quad ، \quad \omega_y = \sqrt{\frac{k_y}{m}}$$
$$، \quad \omega_\theta = \sqrt{\frac{K_{\theta R}}{mr^{\,2}}} \quad ، \quad \Omega = \frac{\omega_\theta}{\omega_y} \tag{4}$$

Where $K_{\theta R}$ is the torsional stiffness, k_x and k_y are the lateral stiffness, ω_θ is the uncoupled torsional frequency, ω_y is the uncoupled lateral frequency.

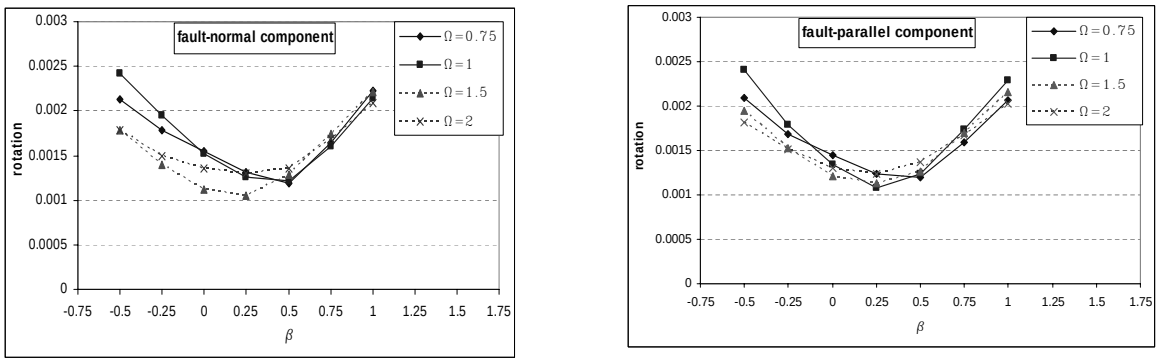

(a) (b)

Fig.7 comparison rotation demands considering actual behavior method under (a) fault-normal and (b) fault-parallel component excitation

In actual methods, elements yield displacement is related to element dimension characteristics and reinforce yield strain. Hence elements with different dimensions would have varied yield displacement. In common behavior method, strength is distributed between elements on the basis of elements stiffness, so all elements would have equal yield displacement. Fig. 7 and Fig. 8 compare the rotational demand considering actual and common behavior methods, respectively, when system subjected to near-fault ground motion. It should be mentioned that in all analysis, near-fault and far-fault components are applied to the system simultaneously. As Figure 7 shows, when fault-normal component excited asymmetric direction, variation trend of the rotational demand would contrary to fault-parallel component. However, for fault-normal and fault-parallel components considering Ω=1 and for β=-0.5, which is maximum stiffness eccentricity, led to the rotational demand would be maximized. For each frequency ratio and both fault-normal and fault-parallel components, when stiffness and strength are located on opposite side of the mass center, the rotational demand conflicted with those which mentioned centers are located on one side of the mass center. The rotational demand values for fault-normal and fault-parallel are approximately similar. As can be seen, for β=0.25 and β=0.5 cases rotational response would be minimized. Moreover, for β=-0.5 and β=1 cases rotational demand, considering different frequency ratios, would be maximized. It could be concluded that, when stiffness and strength centers are located on one side of mass center, rotational response would be maximized.

While, the stiffness and strength centers located on opposite sides of mass center, makes the rotational response to be minimized.

Figure 8 presents rotational demand versus β parameter considering common behavior method. As can be seen, against actual behavior method, rotational demand values for fault-normal component is greater than those of fault-parallel component. The rotational response considering Ω=1 and all β values would be maximized. Response reduction trend would be occurred in 0.75, 1.5 and 2 frequency ratios, respectively. For all frequency ratios, minimum rotational response is occurred for the case of β = -0.5 (i.e. maximum stiffness eccentricity) and minimum response shown for the case of β=1 (i.e. minimum stiffness eccentricity). Furthermore, maximum dispersion of rotational response is happened for the case

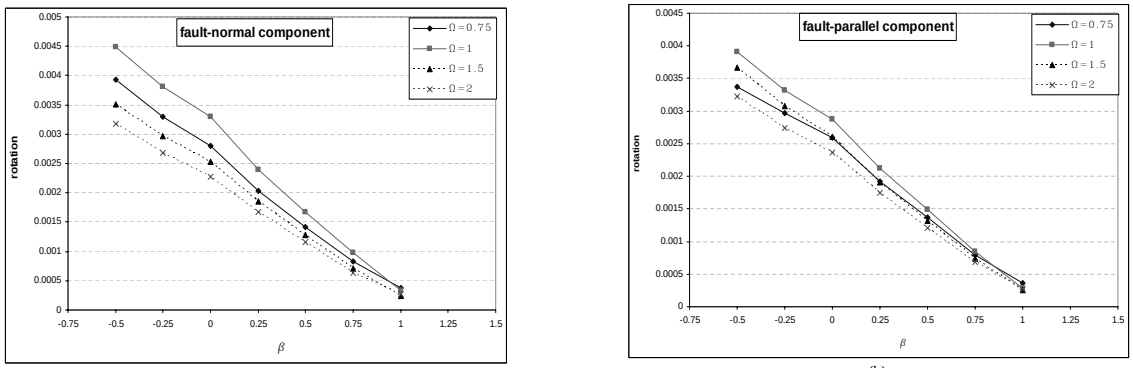

Fig.8 comparison rotation demands considering common behavior method under (a) fault-normal and (b) fault-parallel component excitation

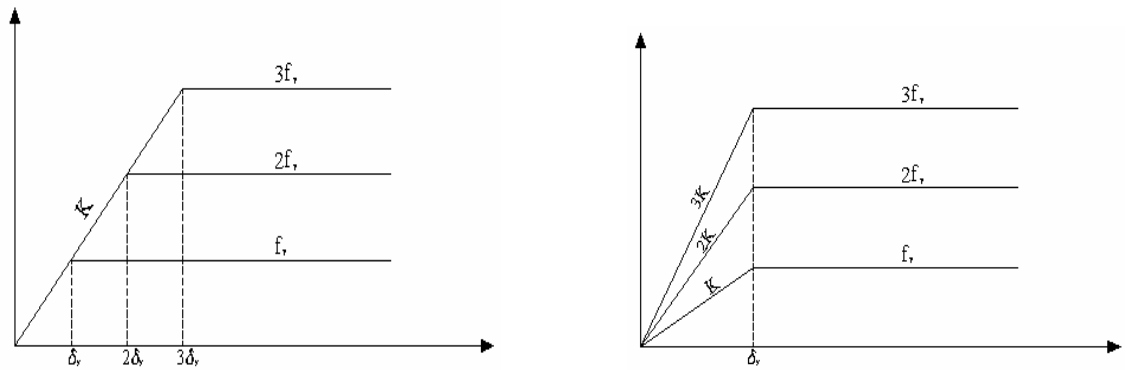

Fig.9 variations in characteristics of element considering (a) actual behavior method and (b) common behavior method

of β=–0.5 and minimum dispersion is occurred for the case of β=1. So, it is revealed that, the major parameter in common behavior method is the stiffness eccentricity.

5.2. Effect of Strength Ratio on Rotational Demand

Figure 9(a) shows the force-displacement relationship in the common behavior method for assigning different strengths. Increasing strength will lead to an increase of yield displacement. However, the stiffness of the element remains unchanged. On the other hand, Figure 9(b) shows the force-displacement relationship in the actual behavior method for assigning different strengths. In this case, the yield displacement would be independent of strength and consequently, the yield displacement remains constant. Nevertheless, the stiffness would be dependent upon the strength.

It is well known that in the common behavior method by increasing strength, inelastic process would be delayed, and the maximum displacement would be smaller than displacements with the lower strength. However, in actual behavior method considering different strengths, the maximum displacement doesn't show noticeable change. Figure 10 presents the rotational demand versus β parameter, considering actual and common behavior methods. Also three strength ratios named as usual, double and triple which represent as

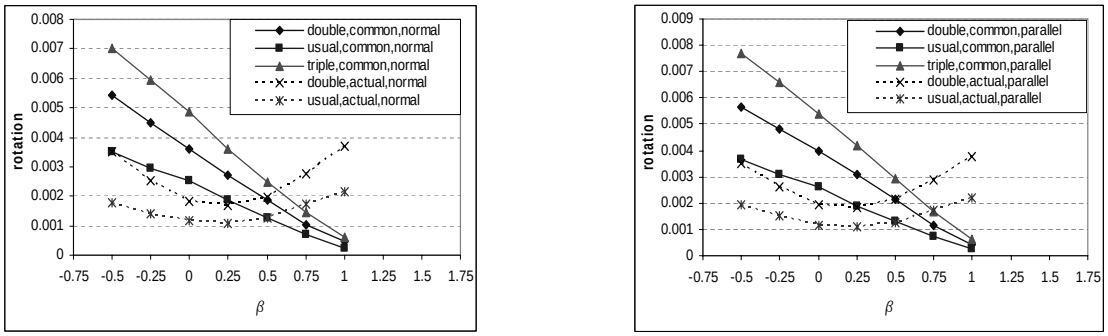

(a) (b)

Fig.10 rotation demands considering different strength in common and actual behavior method under (a) normal component and (b) parallel component excitation

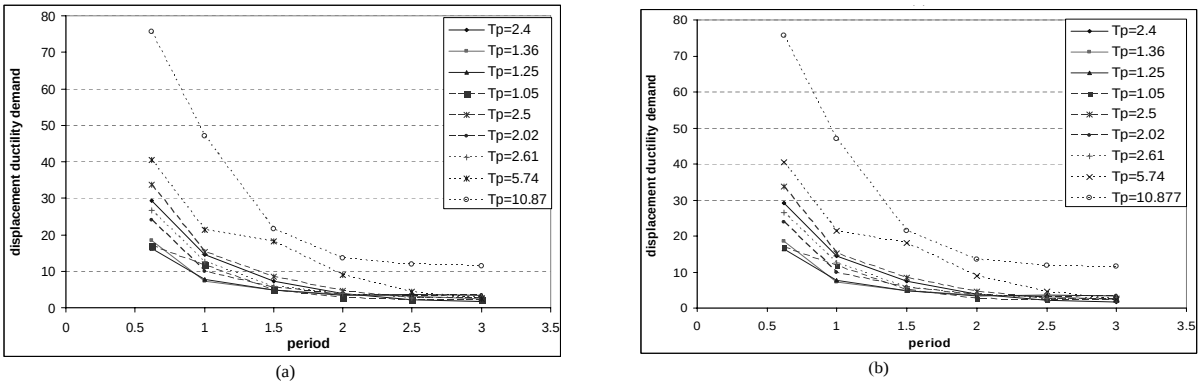

(a) (b)

Fig.11 displacement ductility demands of near-fault motions for (a) constant stiffness case and (b) variable stiffness case

1,2,3 strength ratios respectively and are illustrated in the figure. In Fig. 10(a) y-direction of system subjected to fault-normal component of near-fault motions. While in Fig. 10(b) fault-parallel component excited that direction of system.

In both behavior methods considering strength constant coefficients, stiffness, strength and yield displacement eccentricities don't change, while strength changes, rotation demands would be changed. As can be seen, the rotational demand values for fault-parallel component are greater than those of fault-normal component. For β=0.5 (i.e. strength eccentricity equal stiffness eccentricity which those located on opposite the mass center) the rotational demand either considering common behavior method or actual behavior method are similar. Mentioned issue in both fault-normal and fault-parallel components would valid. The trend of rotation demands changes for strength ratios are similar to the first strength. In actual and common behavior methods, the rotation demands would also increase by increasing strength.

5.3. Effects of Near-Fault Motions on Deformation Demand

The variation of displacement ductility demand versus structural period is shown in Fig. 11 for Ω equals to 1 and T_y equals to 0.62, 1.0, 1.5, 2.0, 2.5 and 3 second. The structural period is achieved either considering constant stiffness or variable stiffness. In the former case, the yield displacement of element would vary and

Table 4 periodic characteristics of fault-normal component of near-fault ground motions

record	Component	T_P	T_{P-v}	T_F
EZ92erzi	Erzinkan- 90	2.4	1.82	2.00
NR94newh	Newhall- 360	1.36	1.3	0.71
NR94rrs	Rinaldi- 228	1.25	1.02	0.91
NR94spva	Sepulveda- 270	1.05	0.84	0.67
NR94scs	Converter- 52	2.5	2.96	1.11
NR94sylm	Olive- 360	2.02	2.6	1.44
NR94sce	East- 18	2.61	0.84	0.84
CH92tcu52	Tcu52- N	5.7	10.2	1.88
CH92tcu68	Tcu68- N	10.875	8.12	7.75

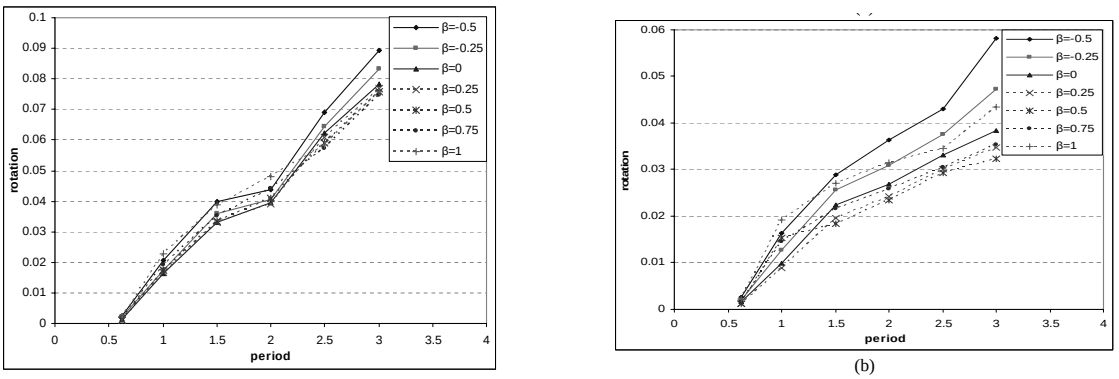

(a) (b)

Fig.12 rotation demands of near-fault motions for (a) constant stiffness case and (b) variablestiffness case

consequently the element dimension would change in order to derive the structural period. In the latter case, the yield displacement of elements as well as stiffness varies in order to achieve the desirable period. The propagation of fault rupture toward a site at a velocity close to the shear wave velocity causes most of the seismic energy from the rupture to arrive in a single large pulse of motion that occurs at the beginning of the record [8]. As it is observable in Table 4, pulse periodic characteristics determine basis different definitions. In most researches pulse period is resulted from velocity time history (T_p). In some studies pulse period is defined as a period relative to maximum velocity spectrum (T_{p-v}). Likewise, the dominated period of earthquake is determined by Fourier amplitude spectrum. Hence, dominated period is also exhibited (T_F) for a comparison with pulse period. In this study, T_p is defined as pulse period of fault-normal component, which is resulted from velocity time history of that component. For constant stiffness, as it can be seen from the figure 11(a), displacement ductility demand would decrease as the structural period increases. However, by increasing the pulse period of fault-normal component, the ductility demand increases too. In shorter structural periods, dispersion of ductility demand is more pronounced than the higher structural period. For the variable stiffness as it can be seen in figure 11(b) almost the similar pattern of variation is visible in comparison with the constant stiffness case. Fig. 12 presents the maximum floor rotation versus structural

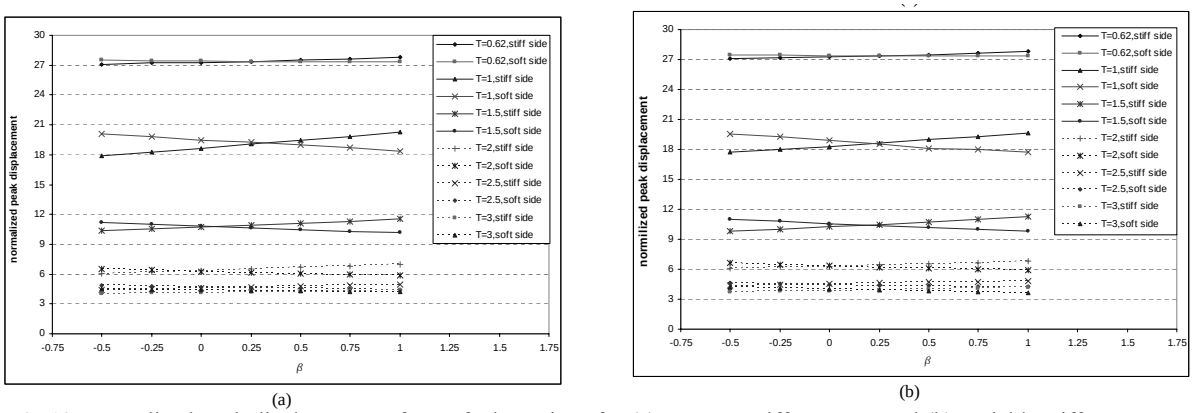

(a) (b)

Fig.13 normalized peak displacement of near-fault motions for (a) constant stiffness case and (b) variable stiffness case

period for different strength eccentricities (i.e. β parameter) and for both constant and variable stiffness cases. Constant stiffness case has larger lateral and torsional stiffness in comparison with variable stiffness case. Considering different structural periods and β values, rotational response for constant stiffness case is larger than variable stiffness case. As it can be seen in the figure, for all the structural period considered in this study, the rotational response would be minimized, when stiffness and strength centers are located on the opposite sides of mass center. For variable stiffness case the rotational response would be minimized in β=0.25 when short periods considered. However for long periods the rotational response in β=0.5 would be minimized. For constant stiffness case, in short periods, minimum rotational response is similar to the prior one while in long periods minimum rotational response is happened for β=0.75. On the other hand, for both variable and constant stiffness cases, for short periods minimum rotational response is created in small strength eccentricity while for long periods it is created in small stiffness eccentricity. Fig. 13 shows the normalized peak displacement versus β parameter for constant and variable stiffness cases and for stiff and soft side elements. The yield displacement of the element located on mass center is used for normalizing. As it can be seen from the figure, the normalized peak displacement values of constant stiffness case are greater than variable stiffness case. It is interesting to note that the system lateral stiffness of the former state is greater than the latter state. Variation pattern of displacement demand is different for stiffness and strength centers located on one side or opposite sides of mass center. In one side location, soft side displacement demand is greater than stiff side. However in the opposite side location, the stiff side displacement demand is greater than soft side which is contrary to the conventional guideline. The stiff side ductility demand is greater than the soft side which is in accordance with the guideline. While reference [8] concluded that for multi-storey of concrete frames, the soft side ductility demand is greater than the stiff side. Figure 14 presents the rotational demand versus T/T_p ratio considering β parameter. Fig. 14(a) is related to constant stiffness case while in Fig. 14(b) variable stiffness case considered. As can be seen, the rotational response would be divided to three regions which related to T/T_p ratio. Within $0 \leqq T/T_p \leqq 0.5$, minimum and maximum rotational response would occur. However, $T/T_p=1$ variation of rotational demand would be minimized. Within $T/T_p \geqq 1$, the rotational demand increases with increasing the stiffness eccentricity. It is observed that in the

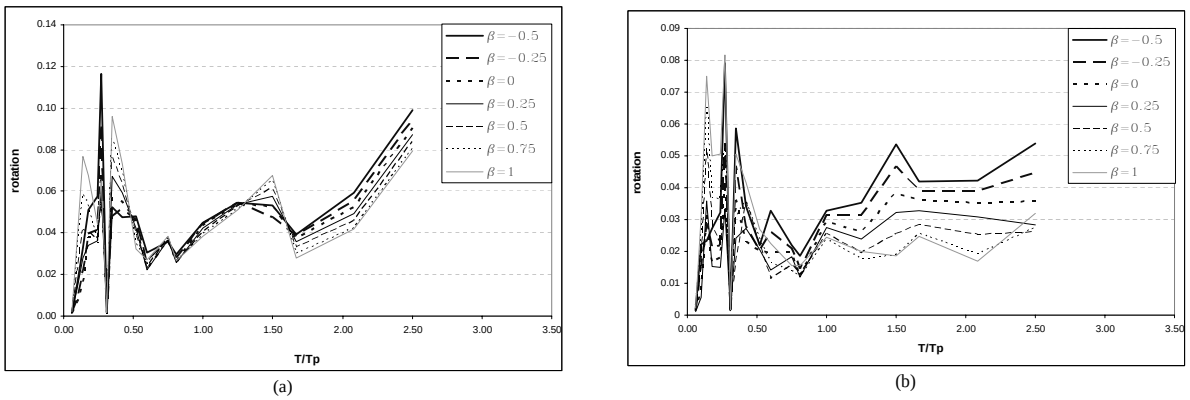

(a) (b)

Fig.14 rotation variation versus T/T_p ratio considering β values for (a) constant stiffness case and (b) variable stiffness case

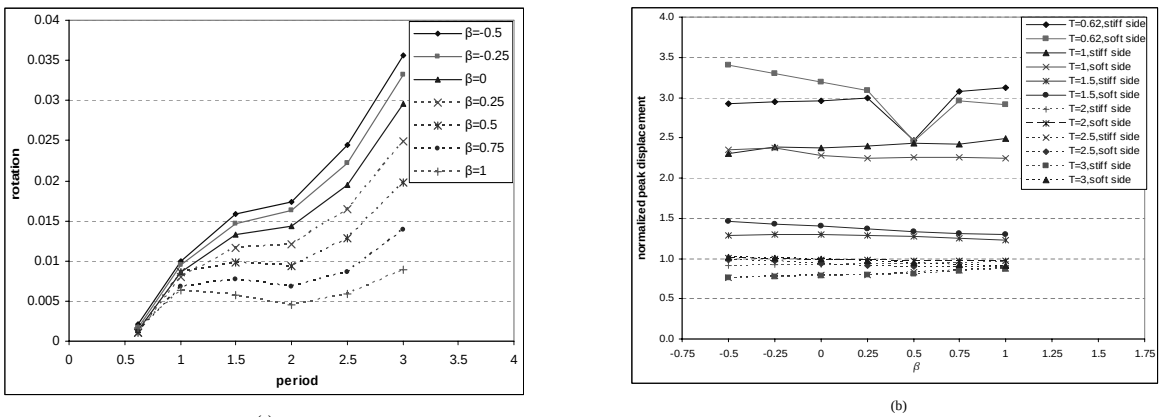

(a) (b)

Fig.15 variation of (a) rotation demands and (b) normalized peak displacement under far-fault ground motions

third region, differences between the rotational demands of variable stiffness case in comparison with those of the constant stiffness case are noticeable.

5.4. Effects of Far-Fault Motions on Deformation Demand

The variation of rotational demand versus structural period for different strength eccentricity (i.e. β parameter) is presented in Fig 15(a). Structural period and frequency ratio is similar to aforesaid values. Because structural responses for constant and variable stiffness cases haven't significant difference, therefore response values presented for one case. As can be seen, rotational demand would be maximized in β=-0.5 which appropriate maximum stiffness eccentricity. Rotational demand for β=1 would be minimized which appropriate minimum stiffness eccentricity. Moreover, maximum dispersion created for β=1 while minimum dispersion in β=-0.5 would created. From mentioned results, would calculate that stiffness eccentricity is effective parameter for rotational response when system subjected to far-fault motions. Therefore in

actual behavior method, variation trend of rotational demand when subjected to far-fault ground motions is similar to common behavior method which near-fault ground motion excite structural system. Fig 15(b) shows normalized peak displacement versus β parameter for stiff and soft side elements. As can be seen, soft side displacement demand is greater than stiff side for all considered structural period except the period equal 1 second. This issue is according to conventional method. Furthermore, displacement ductility demand by increasing structural period would decrease and the stiff side ductility demand is greater than soft side which according to guideline.

6. Summary and Conclusion

Based on the comparison of actual and common nonlinear behavior of wall elements, effects of near-fault and far-fault ground motions on structural responses are considered in this study. The results reported herein provide torsional response of idealized one-storey structure supported by wall elements. The torsional response of the structural system has led to the following conclusions:

- In the common nonlinear behavior method, for Ω =1 and for all β values, the rotational response would be maximized. Because, major parameter in the mentioned behavior is stiffness eccentricity, maximum rotational response is occurred for β=-0.5 while minimum response in β=1 is observed. In the actual nonlinear behavior method, in spite of the large difference in displacement demand of fault-normal and fault-parallel components, the rotational demand in the components are approximately similar. By considering different Ω, the minimum and maximum rotational demand would be created in β=0.25, β=0. 5 and β=-0.5, β=1 respectively.

- In near-fault ground motions, displacement and rotational demand in constant stiffness case is greater than those of variable stiffness. However, deformation demands of far-fault motions are almost similar.

- In near-fault ground motions, the minimum rotational response considering actual behavior method could be achieved, when stiffness and strength centers are located on opposite side of the mass center. However, general trends in the rotational demand with assumption common behavior method for near-fault motions are similar to those of far-fault motions with two type behavior assumption. In the former cases, stiffness eccentricity determines the minimum and maximum rotational response.

- By increasing pulse period of fault-normal component, the displacement ductility demand also increases. Rotational responses would be divided to three regions which related to T/T_p ratio. Within $0 \leqq T/T_p \leqq 0.5$, minimum and maximum rotational response would occur. However, $T/T_p=1$ variation of rotational demand would be minimized. Within $T/T_p \geqq 1$, the rotational demand increases with increasing the stiffness eccentricity.

- In near-fault motions, variation pattern of displacement demand is different when stiffness and strength centers are located on one side or opposite sides of the mass center. In opposite side location, stiff side displacement demand would be greater than that soft side which is contrary to the conventional guidelines. While stiffness and strength centers are located on one side of mass center, similar to far-fault effects on

displacement demands, soft side displacement demand would be greater than that of the stiff side.

7. References

[1] Shakib, H. and Datta, T.K. 1993. Inelastic response of torsionally coupled system to an ensemble of non-stationary ground motion. International Journal of Engineering Structure, 15, 13-20.

[2] Shakib, H. and Tohidi, R.Z. 2002. Evaluation of accidental eccentricity in buildings due to rotational components of earthquake, Journal of Earthquake Engineering, 6,431-445.

[3] Shakib, H. and Fuladgar, A. 2004. Dynamic soil-structure interaction effects on the seismic response of asymmetric buildings, Journal of Soil Dynamics and Earthquake Engineering, 24,379-388.

[4] Hejal, R. and Chopra, A.K. 1989. Earthquake analysis of a class of torsionally coupled buildings, International Journal of Earthquake Engineering and structural Dynamics, 18,305-323.

[5] Pauley, T. 2001. Some design principles relevant to torsional phenomena in ductile buildings, Journal of Earthquake Engineering, Vol. 5, No. 3

[6] Myslimaj, B. and Tso, W.K. 2003. A yield displacement distribution-based approach for strength assignment to lateral force-resisting elements having strength dependent stiffness, International Journal of Earthquake Engineering and structural Dynamics, 32, 2319-2351

[7] Sommer, A. and Bachmann, H. 2005. Seismic behavior of asymmetric RC wall buildings Principles and new deformation – based design method, International Journal of Earthquake Engineering and structural Dynamics, 34,101-124.

[8] Sathopoulso, K.G. and Anagnostopoulos, S.A. 2005. Inelastic torsion of multistorey buildings under Earthquake excitations, International Journal of Earthquake Engineering and structural Dynamics, 34, 1449-1465.

[9] Perus, I. and Fajfar, P. 2005. On inelastic seismic response of asymmetric single structure under bi-axial excitation, International Journal of Earthquake Engineering and structural Dynamics, 34,931-941.

[10] Somerville, P. 1998. Development of an improved representation of near – fault ground motions SMIP98 Seminar on Utilization of Strong – Motion Data: Oakland, California, September 15, 1998, Proceedings, California Division of Mines and Geology, Sacramento, 1998, pp 1-20.

[11] Alavi, B. and Krawinkler, H. 2004. Behavior of moment-resisting frame structures subjected to near- fault ground motions, International Journal of Earthquake Engineering and structural Dynamics, 33,687-706.

[12] Mavroeidis, G.P. and Dong, G. and Papageorgiou, A.S. 2004. Near-fault ground motions and the response of

elastic and inelastic single-degree-of-freedom (SDOF) systems, International Journal of Earthquake Engineering and structural dynamics, 33, 1023-1049.

[13] Edrik, M. and Durukal, E. 2001. A hybrid procedure for the assessment of design basis earthquake ground motions for near-fault conditions, Soil Dynamics and Earthquake Engineering, 21,431-4432.

[14] Chopra, A.K. and Chilntanapakdee, C. 2001. Comparing response of SDF systems to near–fault earthquake motions in the context of spectral regions, International Journal of Earthquake Engineering and Structural Dynamics, 30, 1769-1789

[15] Federal Emergency Management Agency, 2001. NEHRP Recommended Provisions for seismic regulations for new buildings and other structures, 2000 Edition, FEMA 368. FEMA: Washington, DC

[16] Chopra, AK. 2001. Dynamics of Structures: Theory and Applications to Earthquake engineering (2nd edn). Prentice – Hall: Upper Saddle River, NJ.

[17] Pristley, M. and Kowalsky, M. j. 1998. Aspect of drift and ductility capacity of rectangular cantilever structural walls, Bulletin of the New Zealand society for earthquake engineering, Vol. 31, No. 2

[18] Rutenberg, A. 2004. The seismic shear of ductile cantilever wall systems in multistorey structures, International Journal of Earthquake Engineering and structural Dynamics, 33,881-896.